CHEMISTRY
A EUROPEAN JOURNAL

DOI: 10.1002/chem.201103089

# Cyclohexane Ring as a Tool to Select the Presentation of the Carbohydrate Moiety in Glycosyl Amino Acids

**Fernando Rodríguez, Víctor J. Somovilla, Francisco Corzana,* Jesús H. Busto, Alberto Avenoza, and Prof Jesús M. Peregrina*[a]**

**Abstract:** The design of mimic molecules that resemble natural products can be a useful tool to help understand the key aspects in molecular recognition processes that are difficult to access by using natural derivatives. We present the synthesis and the conformational analysis of different glucosylated diamide amino acids that simulate glycopeptides with β-O-linked glucose and contain the nonnatural β-hydroxycyclohexane-α-amino acid. The study, using NMR experiments, X-ray spectroscopy, and molecular dynamics simulations, reveals that the cyclohexane ring allows some naturally occurring ways of presentation of the carbohydrate to be fixed, or to stabilize some novel conformations. In addition, different chair conformations for the cyclohexane-α-amino acid moiety can be set, in particular, those with high population of conformers in which the bulky groups are located at axial positions. Moreover, to increase the scope of these cyclohexane derivatives, two dipeptides incorporating the glycomimics have been synthesized and further glycosylated to obtain the corresponding α-*O*-glycopeptides. These features can have important implications for the design of new drugs and for understanding the complex molecular processes that take place between glycopeptides and their biological targets.

**Keywords:** conformation analysis · glycopeptides · molecular modeling · molecular recognition · NMR spectroscopy

## Introduction

A large number of proteins undergo post-translational modification by glycosylation of amino acids such as serine (Ser) and threonine (Thr). It is well-known that this glycosylation influences some properties of the corresponding proteins such as solubility, stability toward chemical and enzymatic degradation, as well as conformation and folding. It can also affect the biological functions of proteins in events of molecular recognition, for example, cell-to-cell communication and adhesion of bacteria or viruses to cell-surface proteins.[1] In particular, β-*O*-linked attachment of D-glucose (Glc) to Ser/Thr has been found in the epidermal growth factor (EGF) domains of different serum proteins and in Notch receptor (see Figure 1).[2] The role of the Glc moiety in these systems is unknown and remains controversial.

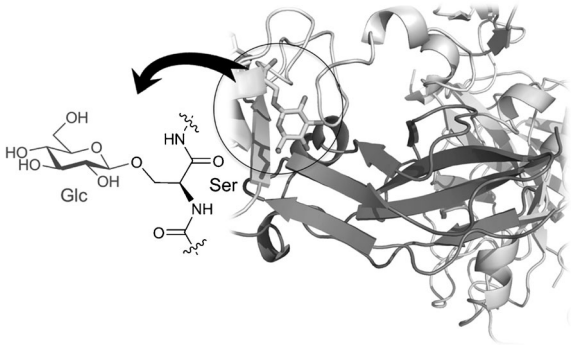


Figure 1. Crystal structure of the complex of the blood coagulation factor VII with a soluble tissue factor (1DAN pdb code)[2e] showing the D-glucose residue attached to a serine of the coagulation factor.

From a structural viewpoint, both the spatial disposition of the sugar moiety with respect to the amino acid and the properties of the underlying amino acid are crucial for successful interaction with the biological targets. In this regard, we have recently reported the different sugar presentation showed by Ser and Thr glycopeptides[3] and its influence on the binding to a synthetically prepared lectin-like receptor.[4]

In addition, it is necessary to study in detail the interactions between the sugar and the underlying amino acid because they play a crucial role in the presentation of the carbohydrate moiety and, consequently, in the interactions with the corresponding biological receptors.

[a] Dr. F. Rodríguez, V. J. Somovilla, Dr. F. Corzana, Dr. J. H. Busto, Prof. A. Avenoza, P. J. M. Peregrina
Departamento de Química
Universidad de La Rioja
Centro de Investigación en Síntesis Química
UA-CSI, Madre de Dios, 51
26006 Logroño (Spain)
Fax: (+34) 941-299-621
E-mail: jesusmanuel.peregrina@unirioja.es
francisco.corzana@unirioja.es

Supporting information for this article is available on the WWW under http://dx.doi.org/10.1002/chem.201103089.

Our group has been involved in the design of new glycopeptides with well-defined conformational preferences.[4,5] In general, our studies conclude that whereas the substituents at carbon $C_\alpha$ affect mainly the conformation of the backbone—forcing it to adopt a helix-like conformation—those present at $C_\beta$ modify the behavior of the glycosidic linkage, particularly the $\psi_s$ dihedral angle, forcing it to adopt an eclipsed conformation. Moreover, these substituents and, in particular, their spatial dispositions, have an important effect on the flexibility of the lateral chain. As a consequence, these custom-made molecules can stabilize conformations present in natural occurring molecules or exhibit some atypical conformations. This feature should be a powerful tool that could be used to design and modulate the conformational space of synthesized glycopeptides and could be useful in determining the structural elements of the natural occurring glycopeptides that are necessary for binding with their biological targets.

With the intention of expanding this outlook to novel systems, we herein report the synthesis and conformational analysis in aqueous solution of the four glucosylated diamide amino acids shown in Figure 2, by combining NMR experiments with molecular dynamics (MD) simulations. In these molecules, Ser or Thr moieties have been replaced by all the possible stereoisomers of the nonnatural β-hydroxycyclohexane-α-amino acid ($c_6$Ser)[6] and the amine and carboxylic acid groups were transformed into amides to simulate a peptide backbone. Additionally, a pivaloyl group was employed, which favors the formation of monocrystals and makes the manipulation of the new compounds easier. It is important to note that the substructure β-*O*-Glc linked to a cyclohexane ring is found in steroidal saponins, which possess anti-inflammatory, hemolytic, cytotoxic, antifungal, and antibacterial properties.[7]

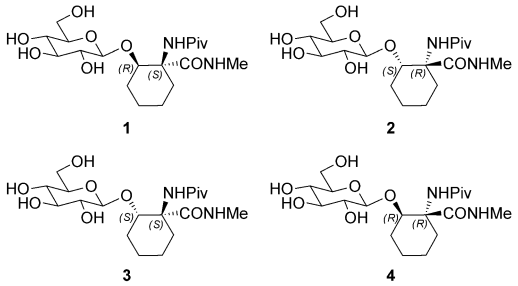


Figure 2. Glucosylated diamide amino acids studied in this work.

## Results and Discussion

**Synthesis**: The synthesis of the final glucosylated diamide amino acids **1**–**4** (Scheme 1) started from the hydrochloride salts of the corresponding 1-amino-2-hydroxycyclohexanecarboxylic acids previously prepared by our group.[6] Thus, treatment of *rac*-**5** with pivaloyl chloride and diisopropylethylamine in dichloromethane led to formation of oxazolone *rac*-**6**, which was opened by methylamine in acetonitrile to form *rac*-**7**. A mixture of the final precursors **8** and **9** was synthesized from *rac*-**7** following a modification of the Koenigs–Knorr glycosylation.[8] The crude reaction product was then purified and separated by column chromatography on silica gel, and single crystals were obtained by slow evaporation from a solution of **9** in diethyl ether/hexane. The crystal structure of **9**, deduced from the X-ray diffraction analysis, confirmed unambiguously its absolute configuration as 1*R*,2*S* (Figure 3). Finally, deprotection of the hydroxyl groups of the carbohydrate moiety with sodium methoxide gave glucosylated diamide compounds **1** and **2**.

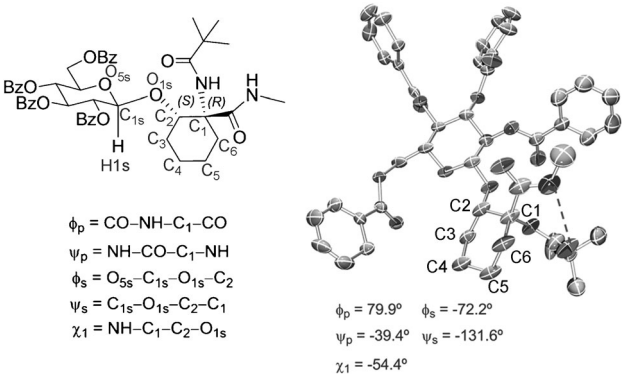


Figure 3. X-ray crystal structure of compound **9**, together with atom labeling and definition of dihedral angles used in this work.

Compounds **3** and **4** were obtained following an identical protocol (Scheme 1). In this case, we could not obtain a crystal structure for any of the intermediates, and the absolute configuration of the glucosylated diamide amino acids was determined by starting the synthesis from the enantiomerically pure (1*R*,2*R*)-1-amino-2-hydroxycyclohexanecarboxylic acid hydrochloride (1*R*,2*R*)-**10**, which led to compound **4** via **14**.

**Conformational study**: Relevant torsion angles and labels of the atoms used in this work for all the compounds are shown in Figure 3.

In a first step, full assignment of the protons in all of the compounds was carried out using COSY and HSQC experiments. Selective 1D NOESY experiments in $D_2O$, and 2D NOESY experiments in $H_2O/D_2O$ (9:1) were then carried out for all compounds (see Figure 4 and the Supporting Information).

The presence of medium NOE cross-peaks between the NH protons of the backbone indicates that the helix-like conformations are significantly populated in the four derivatives.[9] In addition, the strong NOE signal between the anomeric proton H1 s and H2 implies the predominance of the typical *syn* conformation [angle C1 s-O1 s-C2-H2 close to 0°] for the $\psi_s$ glycosidic linkage for compounds **1**–**4**.[5d,10]

The next step was to generate a theoretical ensemble that could reproduce our experimental NMR data. To this end,

  

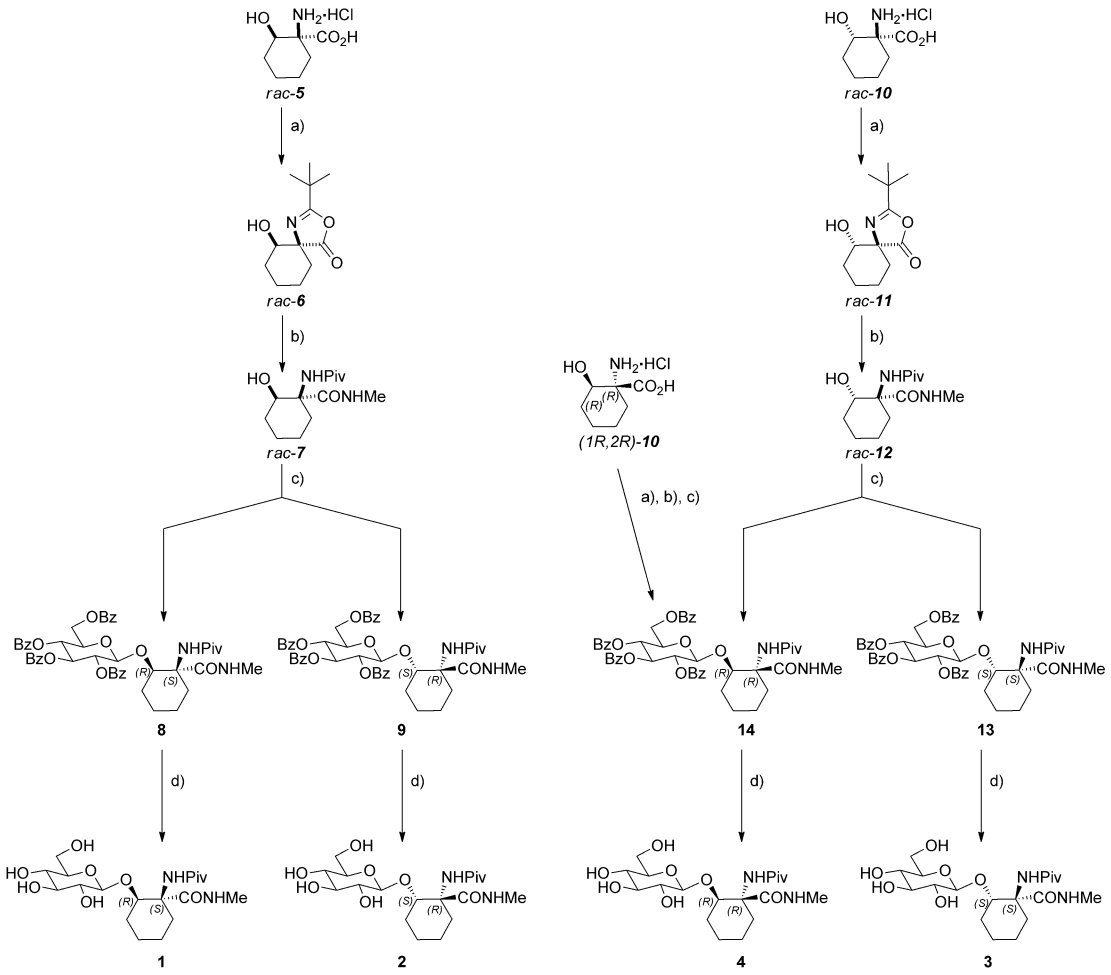


Scheme 1. Synthetic route to glucosylated diamide amino acids **1**–**4**: Reagents and conditions: a) PivCl, DIEA, $CH_2Cl_2$, 0 °C to RT, 16 h, 42 % (*rac*-**11**) and 46 % (*rac*-**6**). b) $MeNH_2$·HCl, DIEA, $CH_3CN$, 70 °C, 24 h, 59 % (*rac*-**7**) and 61 % (*rac*-**12**); c) 2,3,4,6-tetra-*O*-benzoyl-α-D-glucopyranosyl bromide, AgTfO, $CH_2Cl_2$, −30 to 25 °C, molecular sieves 4 Å, 16 h, 36 % (**8**+**9**) and 14 h, 19 % (**13**+**14**); d) MeONa/MeOH, 25 °C, 3 h, 82 % (**1**), 80 % (**2**), 83 % (**3**) and 80 % (**4**).

we used our previously developed protocol,[5,10,11] which combines NMR data with time-averaged restrained MD simulations (MD-tar).[12] Proton–proton distances were experimentally determined from the corresponding NOE build-up curves[13] (see the Supporting Information) and distances involving NH protons were semi-quantitatively determined by integrating the volume of the corresponding cross-peaks. These data were then used as restraints in MD-tar simulations. The distribution for the peptide backbone ($\phi_p$/$\psi_p$), obtained from the MD-tar simulations, is shown in Table 1.

Table 1. Population of the major conformers obtained from the MD-tar simulations for the peptide backbone of glucosylated diamide amino acids **1**–**4**.

| Compound | $\alpha_D$ [%] | $\alpha_L$ [%] | PPII [%] |
|---|---|---|---|
| **1** | 48 | 47 | 3 |
| **2** | 5 | 89 | 4 |
| **3** | 54 | 3 | 42 |
| **4** | 6 | 91 | 3 |

According to the NMR data described above, the four glucosylated diamide amino acids showed a significant population of conformers with $\phi_p$/$\psi_p$ dihedral values that are characteristic of helix-like conformations. However, some important differences can be established among them. Thus, whereas for **1** the MD simulations suggest the existence of a similar population for the two possible helix-like conformations, the $\alpha_L$ (left-handed helix-like) conformer was the most populated in derivatives **2** and **4**. The major conformation of **2** in aqueous solutions is the same as that observed in the solid state for its precursor (**9**, Figure 3). In this case, it is important to note that the crystal structure of **9** showed an inverse γ-turn conformation in the solid state, stabilized by a hydrogen bond between the PivC=O···NHMe groups. In contrast, derivative **3** showed both a PPII (polyproline II) and a helix-like conformation for the peptide backbone. Moreover, whereas derivatives with *R* configuration at Cα (compounds **2** and **4**) tend to adopt the $\alpha_L$ conformation, derivatives **1** and **3** exhibit the $\alpha_D$ (right-handed helix-like) conformer. It is important to mention that these major con-

  

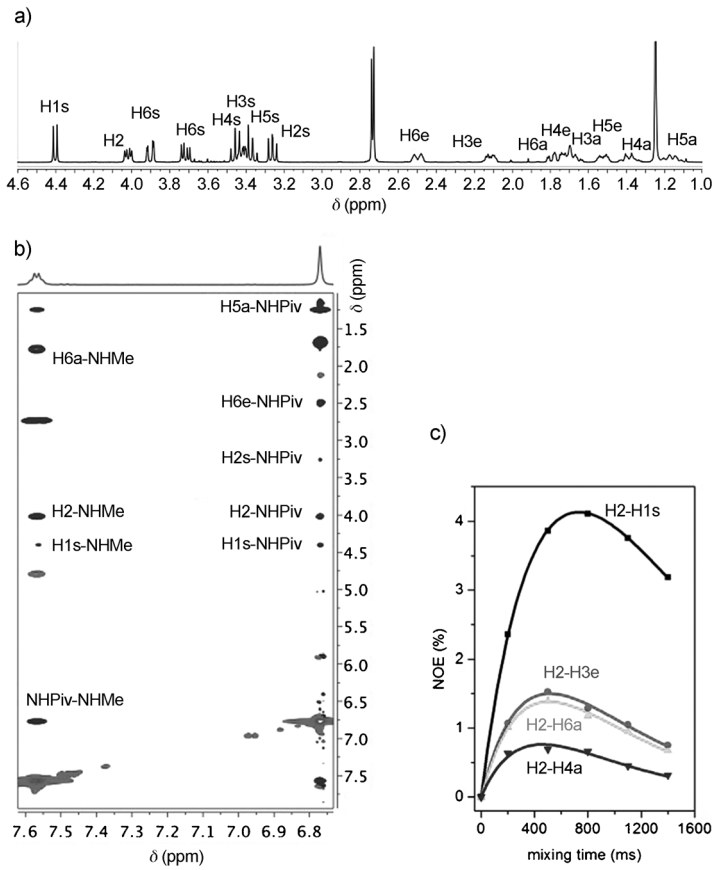


Figure 4. a) $^1$H NMR ($D_2O$); b) 2D-NOESY ($H_2O/D_2O$, 9:1) spectra (400 MHz), and c) selected build-up curves ($D_2O$) for compound **2**. The experiments were run at 25 °C and pH 5.8.

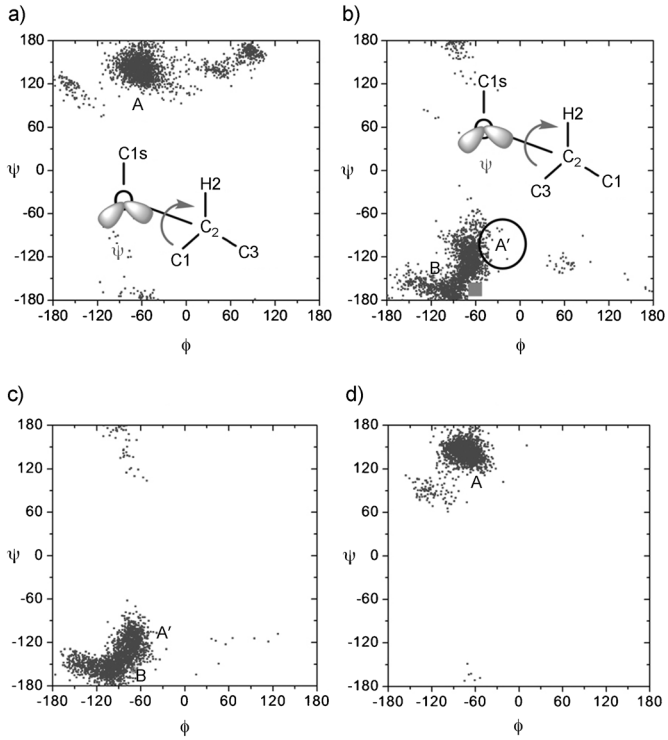


Figure 5. Distribution of the glycosidic linkage ($\phi_s/\psi_s$) of the four glucosylated diamide amino acids obtained from the MD-tar simulations: a) Compound **1**, b) Compound **2**, c) Compound **3**; d) Compound **4**. For compound **2**, the conformation of the glycosidic linkage in the solid state of its precursor (compound **9**) is shown as a square.

formers found for the backbone of the glucosylated diamide amino acids lie at the local minima previously calculated for other α,α-disubstituted amino acids.[5d]

Concerning the glycosidic linkage, $\phi_s$ is mainly determined by the *exo*-anomeric effect,[14] which fixes its value at around −60° in all the derivatives. In addition, neither the stereochemistry at Cα nor the presence of a substituent group at Cα significantly affects the conformation of the glycosidic linkage (Figure 5). In contrast, when a Thr residue is present, the existence of a substituent group at C2 (or Cβ) notably affects the $\psi_s$ torsion angle, which adopts a value close to 120° (compounds **1** and **4**) or −120° (compounds **2** and **3**). This conformation, denoted as A or A' in Figure 5, displays H2−C2 and O1s−C1s bonds in an eclipsed conformation to avoid a nonstabilizing interaction between the cyclohexane ring of the amino acid and the endocyclic oxygen of the carbohydrate moiety. In addition, when C2 adopts the (*S*) configuration (compounds **2** and **3**), the glycosidic linkage becomes more flexible, and a small population of an additional conformer (denoted as B in Figure 5) with $\psi_s$ close to −180° and $\phi_s$ around −120° is also evident. This conformation has also been observed in other nonnatural glycosylated diamide amino acids.[5d]

Inspection of the NOE contacts revealed an interesting equilibrium between the two possible chair conformations for the six-membered ring of the amino acid moiety (Figure 6). In all cases, chair **a** refers to the conformer with the NHPiv group located at an axial position.

From an experimental viewpoint, the equilibrium between the two possible chair conformations can be determined by examining the distances between the H2a and H6a protons deduced from the build-up curves.

Interestingly, in all cases, the most populated chair conformations are those that locates the bulky group (NHPiv) in an axial position (chair **a**), in particular for derivatives **2** and **3**. This result is, to some extent, expected. Indeed, the preference for the amide or amine groups to adopt axial positions in cyclohexane-α-amino acids has been previously reported for the solid state.[15] We also have some crystal structures that corroborate this experimental finding.[16] On the other hand, the results of MD simulations are in good agreement with the experimental data (see the Supporting Information). In compound **2**, with the sugar unit and the NHPiv group in a *cis* relative position, the sugar occupies the equatorial location, which is expected to avoid the 1,3-diaxial interactions. Indeed, chair **a** was also found in the crystal structure of the perbenzoylated compound **9**, which is its precursor. In contrast, for **1**, both chair conformations coexist in aqueous solution with a similar population. Notably, in **3** and **4** the major populated chair conformation (chair **a**) locates the bulky groups (NHPiv and sugar) in axial positions. In this regard, there are some exceptions to the well-estab-

  

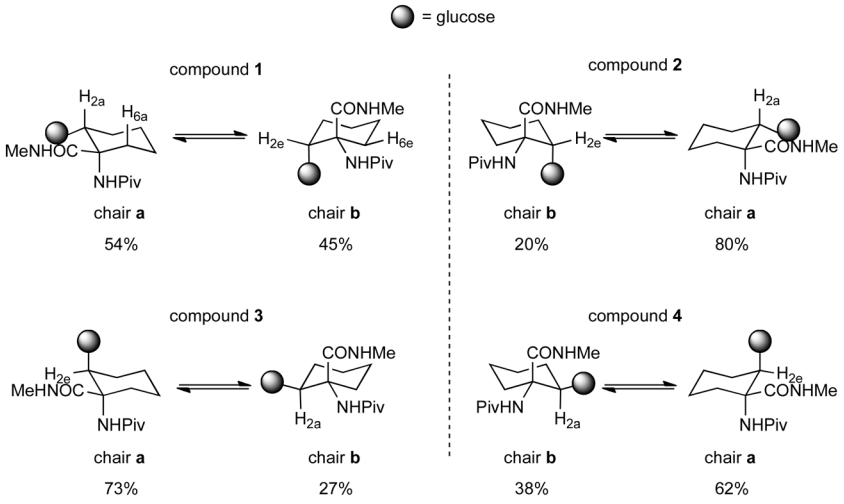


Figure 6. Equilibrium observed in aqueous solution between the two possible chair conformations (denoted as **a** and **b**) of the six-membered ring of the amino acid moiety for the studied glucosylated diamide amino acids.

lished rule that states that, in a cyclohexane ring, the bulky substituents prefer to adopt equatorial positions. One exception is defined as axial/equatorial stability reversal.[17] For example, the sterically crowded all-*trans*-hexaalkylcyclohexane prefers a conformation in which the alkyl groups are located at axial rather than equatorial positions. Moreover, increasing the number and bulk of the alkyl substituent results in a relative stabilization of the axial conformer. The authors suggest that the stability reversal is not due to stabilization of the axial conformer but due to destabilization of the equatorial conformer because of steric and torsional contributions.

As far as the lateral chain is concerned, its conformational behavior is characterized by the $\chi^1$ torsional angle, which can adopt three lowest energy staggered rotamers, denoted as $g(-)$ ($\chi^1 \approx -60°$), $g(+)$ ($\chi^1 \approx +60°$) and *anti* ($\chi^1 \approx 180°$). Figure 7 shows the population of $\chi^1$ obtained from the MD-tar simulations for all the glucosylated diamide amino acids **1**–**4**. For these systems, one should expect a rigid $\chi^1$ due to the restriction imposed by the six-membered ring. The different $\chi^1$ values observed for each molecule are related to the equilibrium described above between the two possible chair conformations of the amino acid ring.

Thus, for compounds **1** and **4**, with a significant presence of both chair conformations in solution, the lateral chain is quite flexible, with two possible values: $g(+)$ and $g(-)$ conformations for derivative **1** and $g(-)$ and *anti* for compound **4**. In contrast, derivative **2** and especially compound **3**, exhibited $\chi^1$ values corresponding to $g(-)$ and *anti*, respectively. In addition, as can be seen in Figure 7, compounds **3** and **4** showed a clear preference for the *anti* conformation of the lateral chain. An important consequence of this feature is that whereas derivatives **1** and **2** present the carbohydrate moiety in a perpendicular disposition with respect to the backbone, derivatives **3** and **4** present the sugar unit almost parallel to the peptide sequence (Figure 8).

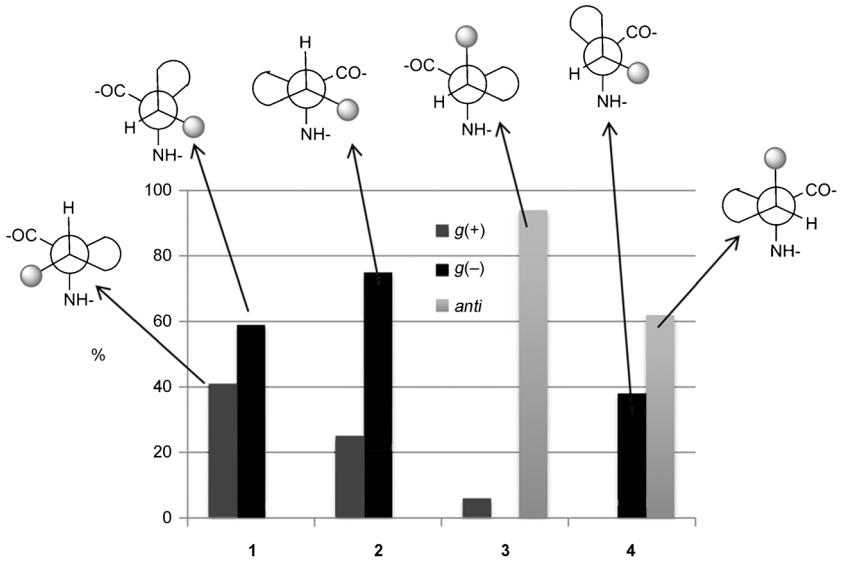


Figure 7. Lateral chain distribution ($\chi^1$) of the four glucosylated diamide amino acids obtained from the MD-tar simulations.

In previous works, we have demonstrated that whereas for the β-Glc-Ser derivatives the carbohydrate and the peptide moieties exhibit a perpendicular disposition, it shifts towards a parallel arrangement in the β-Glc-Thr compounds. On this basis, we could state that cyclohexane derivatives **1** and **2** mimic the conformational behavior of the Ser glycopeptides, whereas compounds **3** and **4** imitate the behavior of the Thr-containing glycopeptides.

To investigate whether these conformations were stabilized by interactions between the peptide and sugar moieties, a hydrogen-bond analysis was carried out; however, in all cases, very weak hydrogen bonds (less than 10% population) were obtained between the two parts of the molecule.

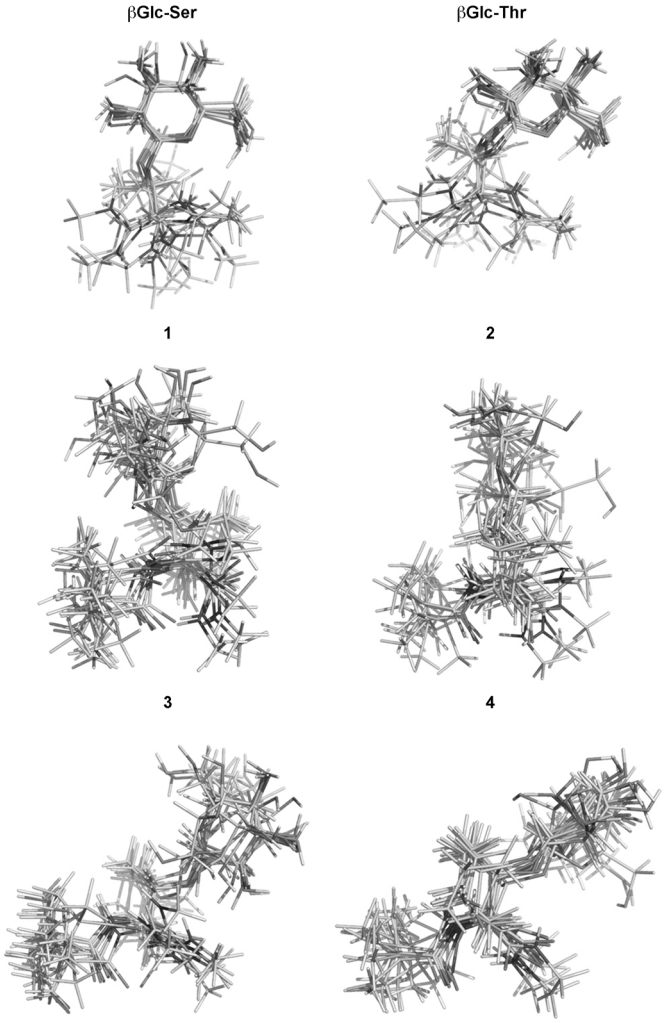


Figure 8. Snapshots taken from the 80 ns MD-tar trajectories collected for the different glucosylated diamide amino acids.

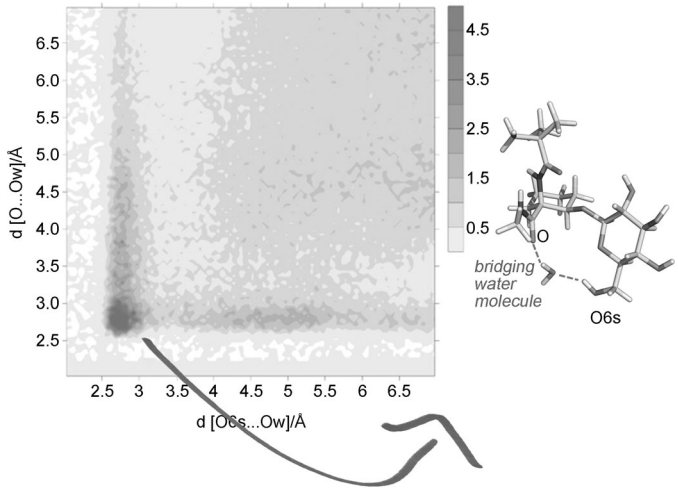


Figure 9. Two-dimensional radial pair distribution function for O6s and O found for compound **1** in the 20 ns unrestrained MD simulation in explicit water.

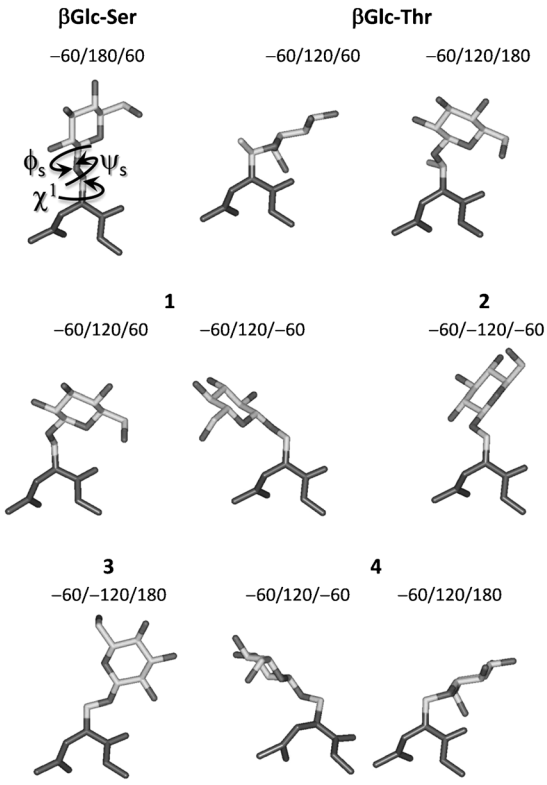


Figure 10. $\phi_s/\psi_s/\chi^1$ values obtained from the MD-tar simulations for the most populated conformers of the glucosylated diamide amino acids **1**–**4**, together with conformers previously deduced for the natural derivatives with Ser and Thr. The configuration of the substituents at the cyclohexane ring can modulate the orientation of the sugar moiety with respect to the underlying amino acid (lower part of the molecules; shown in dark grey). The cyclohexane ring has been removed for clarity.

Therefore, taking into account the influence that the water molecules could exhibit on the conformation of the glucosylated diamide amino acids, the anisotropic hydration of the solutes was inspected. To this end, the normalized, one-dimensional and two-dimensional radial pair distributions[18] were calculated from the 20 ns unrestrained MD simulations carried out in explicit solvent on the four compounds for all possible shared water density sites. Notably, only for compound **1** was a significant intra-residue water bridge found between atoms O6s and the carbonyl oxygen of the underlying amino acid (Figure 9). This water pocket was present for about 50% of the total trajectory time, coinciding with the $g(+)$ conformation for the lateral chain, exhibits a very high maximum density (about 7.6 times the bulk density), and differs from that previously found for its natural analogue (βGlc-Ser diamide).[10]

Figure 10 shows the major conformations found for the glucosylated diamide amino acids in aqueous solution studied in this work. As can be seen, several presentations of the carbohydrate moiety with respect to the underlying amino acid are possible using the cyclohexane ring. Thus, for example, compound **4** exhibits one of the major conformers occurring in the natural βGlc-Thr derivative (see compound **4** in Figure 10) and stabilizes an unusual conformation that is not observed in Nature. These geometries

  

might well be used to enhance the binding between the carbohydrate and its biological target. Consequently, the diverse 3D disposition of the sugar could have important implications for drug design. The conformers derived from these systems could also be useful in defining the pivotal elements that are necessary for molecular recognition processes.

To demonstrate the scope of the approach developed in this work, we have incorporated some of the nonnatural amino acids developed above into short peptides: (1*R*,2*R*)-$c_6$Ser-L-Pro and (1*S*,2*S*)-$c_6$Ser-L-Pro. The terminal amino and carboxylic acid groups of these dipeptides were transformed into amides to simulate larger peptides. These dipeptides were treated with tri-*O*-benzyl-2-nitro-D-galactal and potassium *tert*-butoxide to obtain the corresponding α-anomers, thus demonstrating that this kind of nonnatural amino acid can be used to form both α- and β-glycosidic bonds in the glycosylation reactions. Their syntheses and spectroscopic data are collected in the Supporting Information. Fortunately, it was possible to obtain the crystal structure of compound **15**, which corresponded to PivNH-(1*R*,2*R*)-$c_6$Ser*-L-Pro-CONHMe, in which (*) refers to the glycan moiety indicated in Figure 11. As can be seen in Figure 11, the backbone adopts a type II′ β-turn and the glycosidic linkage exhibits the typical eclipsed conformation, with $\psi_s$ around 140°. As also occurs for its analogue, compound **4**, the cyclohexane ring of **15** mainly adopts the chair **a** conformation, with the bulky groups located at axial positions. Additionally, the conformational behavior of **15** in $CHCl_3$ solution was analyzed by combining NMR data (NOE cross-peaks) and MD-tar simulations (see the Supporting Information for details). Whereas the chair **a** conformation is entirely populated in solution, and the glycosidic linkage mainly shows the eclipsed conformer, the β-turn structure of the peptide backbone coexisted with typical helix-like conformations forced by the $c_6$Ser residue in a 3:1 ratio, respectively.

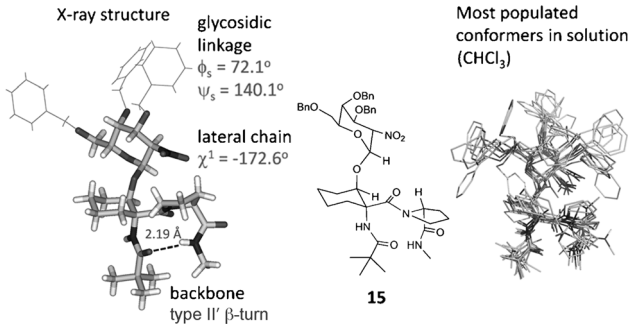


Figure 11. X-ray crystal structure (left) and most populated conformers found in solution (right) for compound **15**.

Finally, in future work, we would like to introduce all these derivatives into larger glycopeptides with the aim of enabling them to be recognized by biological targets. To test the viability of this idea, MD simulations were run to investigate the interactions between these novel glucosylated diamide amino acids and a lectin that recognizes glucose. Although there are different systems that recognize glucose, such as *lens culinaris* lectin[19] or the *E. coli* glucose/galactose chemoreceptor protein,[20] GRFT protein[21] was chosen for this purpose because it exhibits potent antiviral activity against human immunodeficiency virus (HIV) by binding to viral envelope glycoproteins. Surprisingly, this high activity can be inhibited by low concentrations of mannose, *N*-acetylglucosamine (GlcNAc), and glucose, which makes it interesting to study in detail the molecular recognition process of these monosaccharides by GRFT.

All the simulations were started from the crystal structure of the complex between GRFT and glucose (PDB code: 2NUO). In our case, and at least from a theoretical viewpoint, all the glucosylated diamide amino acids exhibited the same interactions with lectin (see Figure 12). This result could be explained by the fact that O1 and O2 point away from the protein chain and also corroborates the experimental finding that lectin recognizes, in a similar way, mannose, GlcNAc, and glucose.

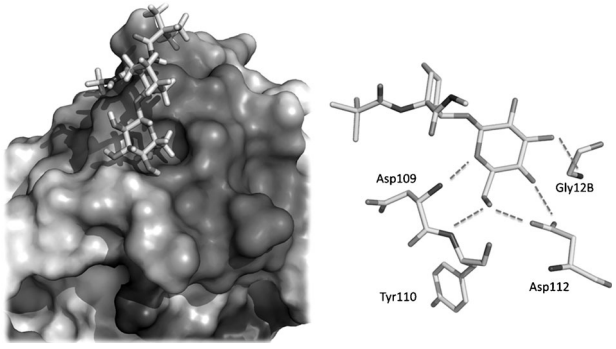


Figure 12. Details of the interactions between compound **4** and site 1 of the antiviral protein griffithsin (GRFT), as deduced from unrestrained 20 ns MD simulations in explicit water.

## Conclusion

The synthesis and conformational analysis of glycosylated diamide amino acids with β-*O*-linked glucose and containing the nonnatural β-hydroxycyclohexane-α-amino acid residue have been investigated. The study, which combines NMR experiments, X-ray spectroscopy, and molecular dynamics simulations, reveals that the cyclohexane ring can effectively modulate the presentation of the sugar moiety with respect to the underlying amino acid residue. These features, together with the fact that the amino acid moiety exhibits different chair conformations for the six-membered ring, allow the molecule to adopt novel conformations that are not found in natural derivatives. Furthermore, two dipeptides incorporating the new derivatives have been synthesized and further glycosylated to obtain the corresponding α-*O*-glycopeptides. The development of these nonnatural derivatives could have important implications for the design of new drugs and for

  

understanding the complex molecular processes between glycopeptides and their biological targets.

## Experimental Section

**General Procedures**: Solvents were purified according to standard procedures. Analytical TLC was performed using Polychrom SI F254 plates. Column chromatography was performed using Silica gel 60 (230–400 mesh). $^1$H and $^{13}$C NMR spectra were recorded with Bruker ARX 300 and Bruker AVANCE 400 spectrometers. $^1$H and $^{13}$C NMR spectra were recorded in $CDCl_3$ with TMS as internal standard or in $D_2O$ (chemical shifts referenced to the internal solvent signals and reported in ppm on the $\delta$ scale; coupling constants in Hz). Assignment of all separate signals for the final compounds in the $^1$H NMR spectra was made on the basis of coupling constants, ge-COSY and ge-HSQC experiments with a Bruker AVANCE 400 spectrometer. The NMR data were processed with Mestre Nova software (Mestrelab Research, Spain). Melting points were determined with a Büchi SMP-20 melting point apparatus. Microanalyses were carried out with a CE Instruments EA-1110 analyzer and are in good agreement with the calculated values. Optical rotations were measured with a Perkin–Elmer 341 polarimeter. Electrospray mass spectra were recorded with a microTOF-Q-BRUKER connected to a Waters 996 photodiode array detector with $H_2O$ or MeOH as carrier solvents. The synthetic procedures for all new compounds as well as their physical properties are detailed in the Supporting Information.

**NMR experiments**: NMR experiments were recorded with a Bruker Avance 400 spectrometer at 298 K. Magnitude-mode ge-2D COSY spectra were recorded with gradients and using the cosygpqf pulse program with 90 degree pulse width. Phase-sensitive ge-2D HSQC spectra were recorded using *z*-filter and selection before t1, removing the decoupling during acquisition by use of invigpndph pulse program with CNST2 (JHC) = 145. 2D NOESY experiments were made using phase-sensitive ge-2D NOESY with WATERGATE for $H_2O/D_2O$ (9:1) spectra. Selective ge-1D NOESY experiments were carried out using the 1D-DPFGE NOE pulse sequence. NOE intensities were normalized with respect to the diagonal peak at zero mixing time. Experimental NOEs were fitted to a double exponential function, $f(t)=p_0\,(e^{-p_1t})(1-e^{-p_2t})$ with $p_0$, $p_1$, and $p_2$ being adjustable parameters.[13] The initial slope was determined from the first derivative at time $t=0$, $f(0)=p_0p_2$. From the initial slopes, interproton distances were obtained by employing the isolated spin pair approximation.

**MD simulations in explicit water**: Simulations were performed by using the AMBER 9 program package (parm99),[22] which was implemented with GLYCAM 06 parameters.[23] Unrestrained MD simulations were carried out in the presence of explicit TIP3P water molecules.[24] RESP atomic charges[25] for the glycopeptides were derived by applying the RESP module of AMBER to the HF/6–31G(d) ESP charges calculated with Gaussian 08.[26] The simulations were run with the PMEMD module of AMBER with SHAKE algorithm,[27] using periodic boundary conditions, a 2 fs time step, a temperature of 300 K, a Langevin type thermostat for temperature control, and constant pressure of 1 atm. A 9 Å cutoff was applied to the Lennard-Jones interactions, and Ewald sums for the treatment of the electrostatic interactions.[28] An initial 2500 cycles of minimization (combining steepest descent with conjugate gradient) were run on both systems by first restraining the atoms of the complex. The whole system was then minimized using 2000 cycles. This first step was followed by 200 ps of dynamics at constant volume with weak positional restrains on the complex (10 kcal mol$^{-1}$·Å2). In this step, the system was heated from 100 to 300 K. The restrains on the solute were removed and 200 ps MD simulations were run at 300 K and 1 atm to obtain the appropriate density. Finally, 20 ns MD simulations were run using the conditions mentioned above.

**MD simulations**: NOE-derived distances were included as time-averaged distance restraints, and scalar coupling constants ($J$) as time-averaged coupling restraints. A $<r^{-6}>^{-1/6}$ average was used for the distances and a linear average was used for the coupling constants. Final trajectories were run using an exponential decay constant of 8 ns and a simulation length of 80 ns.

**X-Ray diffraction analysis**[29]: *Crystal data for 9*: $C_{47}H_{50}N_2O_{12}$; $M_w$ = 834.89; colorless prism of 0.25 × 0.25 × 0.22 mm; $T$ = 173 K; monoclinic; space group $P2_1/c$; $Z$ = 2; $a$ = 13.5848(4) Å, $b$ = 11.7140(3) Å, $c$ = 14.9527(4) Å, $\beta$ = 112.8678(10)°; $V$ = 2192.44(10) Å$^3$; $d_{calc}$ = 1.265 g cm$^{-3}$; $F(000)$ = 884; $\lambda$ = 0.71073 Å ($Mo_{K\alpha}$); $\mu$ = 0.091 mm$^{-1}$; Nonius kappa CCD diffractometer, $\theta$ range 3.43–28.15°, 18857 collected reflections, 9792 unique, full-matrix least-squares (SHELXL97),[30] $R_1$ = 0.0535, $\omega R_2$ = 0.1128, ($R_1$ = 0.0874, $\omega R_2$ = 0.1302 all data), goodness of fit = 1.014, residual electron density between 0.23 and −0.245e Å$^{-3}$. Hydrogen atoms fitted at theoretical positions.

*Crystal data for compound 15·Et$_2$O*: $C_{49}H_{68}N_4O_{11}$; $M_w$ = 889.08; colorless prism of 0.27 × 0.15 × 0.12 mm; $T$ = 173 K; monoclinic; space group $P2_1$; $Z$ = 2; $a$ = 12.2297(6) Å, $b$ = 15.0023(8) Å, $c$ = 13.3856(5) Å, $\beta$ = 98.902(3)°; $V$ = 2426.3(2) Å$^3$; $d_{calc}$ = 1.217 g cm$^{-3}$; $F(000)$ = 956; $\lambda$ = 0.71073 Å ($Mo_{K\alpha}$); $\mu$ = 0.086 mm$^{-1}$; Nonius kappa CCD diffractometer, $\theta$ range 2.05–28.08°, 21769 collected reflections, 5820 unique, full-matrix least-squares (SHELXL97),[30] $R_1$ = 0.0618, $\omega R_2$ = 0.0990, ($R_1$ = 0.1254, $\omega R_2$ = 0.1166 all data), goodness of fit = 1.047, residual electron density between 0.293 and −0.179e Å$^{-3}$. Hydrogen atoms fitted at theoretical positions.

## Acknowledgements

We thank the Ministerio de Ciencia e Innovación and FEDER (project CTQ2009–13814/BQU and FPI grant of V. J. S.), the Universidad de La Rioja (project EGI10/65), and the Gobierno de La Rioja (Colabora 2010/05). F. R. thanks the CSIC for his JAE-Doc Program contract. We also thank CESGA for computer support.

[1] a) R. A. Dwek, *Chem. Rev.* **1996**, *96*, 683–720; b) A. Varki, *Glycobiology* **1993**, *3*, 97–130; c) D. H. Williams, *Nat. Prod. Rep.* **1996**, *13*, 469–478; d) D. F. Wyss, G. Wagner, *Curr. Opin. Biotechnol.* **1996**, *7*, 409–416; e) T. Buskas, S. Ingale, G.-J. Boons, *Glycobiology* **2006**, *16*, 113R-136R; f) C. R. Bertozzi, L. L. Kiessling, *Science* **2001**, *291*, 2357–2364; g) M. R. Pratt, C. R. Bertozzi, *Chem. Soc. Rev.* **2005**, *34*, 58–68.

[2] a) L. Shao, Y. Luo, D. J. Moloney, R. S. Haltiwanger, *Glycobiology* **2002**, *12*, 763–770; b) R. J. Harris, M. W. Spellman, *Glycobiology* **1993**, *3*, 219–224; c) K. Brückner, L. Perez, H. Clausen, S. Cohen, *Nature* **2000**, *406*, 411–415; d) D. J. Moloney, L. H. Shair, F. M. Lu, J. Xia, R. Locke, K. L. Matta, R. S. Haltiwanger, *J. Biol. Chem.* **2000**, *275*, 9604–9611; e) D. W. Banner, A. D′Arcy, C. Chene, F. K. Winkler, A. Guha, W. H. Konigsberg, Y. Nemerson, D. Kirchhofer, *Nature*, **1996**, *380*, 41–46.

[3] F. Corzana, J. H. Busto, G. Jiménez-Osés, M. García de Luis, J. L. Asensio, J. Jiménez-Barbero, J. M. Peregrina, A. Avenoza, *J. Am. Chem. Soc.* **2007**, *129*, 9458–9467.

[4] F. Corzana, A. Fernández-Tejada, J. H. Busto, G. Joshi, A. P. Davis, J. Jiménez-Barbero, A. Avenoza, J. M. Peregrina, *ChemBioChem* **2011**, *12*, 110–117.

[5] a) A. Fernández-Tejada, F. Corzana, J. H. Busto, G. Jiménez-Osés, J. Jiménez-Barbero, A. Avenoza, J. M. Peregrina, *Chem. Eur. J.* **2009**, *15*, 7297–7301; b) A. Fernández-Tejada, F. Corzana, J. H. Busto, A. Avenoza, J. M. Peregrina, *Org. Biomol. Chem.* **2009**, *7*, 2885–2893; c) A. Fernández-Tejada, F. Corzana, J. H. Busto, A. Avenoza, J. M. Peregrina, *J. Org. Chem.* **2009**, *74*, 9305–9313; d) A. Fernández-Tejada, F. Corzana, J. H. Busto, G. Jiménez-Osés, J. M. Peregrina, A. Avenoza, *Chem. Eur. J.* **2008**, *14*, 7042–7058; e) F. Corzana, J. H. Busto, M. García de Luis, A. Fernández-Tejada, F. Rodríguez, J. Jiménez-Barbero, A. Avenoza, J. M. Peregrina, *Eur. J. Org. Chem.* **2010**, 3525–3532; f) F. Corzana, J. H. Busto, F. Marcelo, M. García de Luis, J. L. Asensio, S. Martín-Santamaría, J. Jiménez-Barbero, A. Avenoza, J. M. Peregrina, *Chem. Eur. J.* **2011**, *17*, 3105–3110; g) F. Corzana, J. H. Busto, F. Marcelo, M. García de Luis, J. L. Asensio, S.

  

Martín-Santamaría, Y. Sáenz, C. Torres, J. Jiménez-Barbero, A. Avenoza, J. M. Peregrina, *Chem. Commun.* **2011**, *47*, 5319–5321.
[6] A. Avenoza, J. I. Barriobero, C. Cativiela, M. A. Fernández-Recio, J. M. Peregrina, F. Rodríguez, *Tetrahedron* **2001**, *57*, 2745–2755.
[7] a) V. L. Challinor, P. Y. Hayes, P. V. Bernhardt, W. Kitching, R. P. Lehmann, J. J. De Voss, *J. Org. Chem.* **2011**, *76*, 7275–7280; b) S. G. Sparg, M. E. Light, J. J. vanStaden, *J. Ethnopharmacol.* **2004**, *94*, 219–243.
[8] S. Hanessian, J. Banoub, *Carbohydr. Res.* **1977**, *53*, C13-C16.
[9] H. J. Dyson, P. E. Wright, *Annu. Rev. Biophys. Biophys. Chem.* **1991**, *20*, 519–538.
[10] F. Corzana, J. H. Busto, S. B. Engelsen, J. Jiménez-Barbero, J. L. Asensio, J. M. Peregrina, A. Avenoza, *Chem. Eur. J.* **2006**, *12*, 7864–7871.
[11] F. Corzana, J. H. Busto, G. Jiménez-Osés, J. L. Asensio, J. Jiménez-Barbero, J. M. Peregrina, A. Avenoza, *J. Am. Chem. Soc.* **2006**, *128*, 14640–14648.
[12] a) A. P. Nanzer, T. Huber, A. E. Torda, W. F. van Gunsteren, *J. Biomol. NMR* **1996**, *8*, 285–291; b) A. E. Torda, R. M. Scheek, W. F. van Gunsteren, *J. Mol. Biol.* **1990**, *214*, 223–235; c) D. A. Pearlman, P. A. Kollman, *J. Mol. Biol.* **1991**, *220*, 457–479.
[13] T. Haselhorst, T. Weimar, T. Peters, *J. Am. Chem. Soc.* **2001**, *123*, 10705–10714.
[14] G. R. J. Thatcher, *The Anomeric Effect and Associated Stereoelectronic Effects*, American Chemical Society, Washington, DC **1993**.
[15] a) P. G. Vasudev, R. Rai, N. Shamala, P. Balaram, *Biopolymers* **2008**, *90*, 138–150; b) M. Lasa, A. I. Jiménez, M. M. Zurbano, C. Cativiela, *Tetrahedron Lett.* **2005**, *46*, 8377–8380.
[16] a) A. Avenoza, J. H. Busto, C. Cativiela, J. M. Peregrina, F. Rodrı'guez, *Tetrahedron Lett.* **2002**, *43*, 1429–1432; b) A. Avenoza, C. Cativiela, M. A. Fernández-Recio, J. M. Peregrina, *J. Chem. Soc. Perkin Trans. 1* **1999**, 3375–3379.
[17] a) O. Golan, Z. Goren, S. E. Biali, *J. Am. Chem. Soc.* **1990**, *112*, 9300–9307; b) Z. Goren, S. E. Biali, *J. Am. Chem. Soc.* **1990**, *112*, 893–894.
[18] a) C. Andersson, S. B. Engelsen, *J. Mol. Graphics Modell.* **1999**, *17*, 101–105. b) F. Corzana, M. S. Motawia, C. H. Du Penhoat, S. Perez, S. M. Tschampel, R. J. Woods, S. B. Engelsen, *J. Comput. Chem.* **2004**, *25*, 573–586.
[19] R. Loris, F. Casset, J. Bouckaert, J. Pletinckx, M. H. Dao-Thi, F. Poortmans, A. Imberty, S. Perez, L. Wyns, *Glycoconjugate J.* **1994**, *11*, 507–517.
[20] N. K. Vyas, M. N. Vyas, F. A. Quiocho, *Science* **1988**, *242*, 1290–1295.
[21] a) N. E. Ziolkowska, S. R. Shenoy, B. R. O'Keefe, A. Wlodawer, *Protein Sci.* **2007**, *16*, 1485–1489; b) N. E. Ziolkowska, S. R. Shenoy, B. R. O'Keefe, J. B. McMahon, K. E. Palmer, R. A. Dwek, M. R. Wormald, A. Wlodawer, *Proteins Struct. Funct. Bioinf.* **2007**, *67*, 661–670.
[22] AMBER 9, D. A. Case, T. A. Darden, T. E. Cheatham III, C. L. Simmerling, J. Wang, R. E. Duke, R. Luo, K. M. Merz, Jr. D. A. Pearlman, M. Crowley, R. C. Walker, W. Zhang, B. Wang, S. Hayik, A. E. Roitberg, G. Seabra, K. F. Wong, F. Paesani, X. Wu, S. Brozell, V. Tsui, H. Gohlke, L. Yang, C. Tan, J. Mongan, V. Hornak, G. Cui, P. Beroza, D. H. Mathews, C. E. A. F. Schafmeister, W. S. Ross, P. A. Kollman, University of California, San Francisco, **2006**.
[23] K. N. Kirschner, A. B. Yongye, S. M. Tschampel, J. González-Outeiriño, C. R. Daniels, B. L. Foley, R. J. Woods, *J. Comput. Chem.* **2008**, *29*, 622–655.
[24] W. L. Jorgensen, J. Chandrasekhar, J. D. Madura, R. W. Impey, M. L. Klein, *J. Chem. Phys.* **1983**, *79*, 926–935.
[25] C. I. Bayly, P. Cieplak, W. D. Cornell, P. A. Kollman, *J. Phys. Chem.* **1993**, *97*, 10269–10280.
[26] Gaussian 98, M. J. Frisch, G. W. Trucks, H. B. Schlegel, G. E. Scuseria, M. A. Robb, J. R. Cheeseman, V. G. Zakrzewski, J. A. Montgomery, Jr. R. E. Stratmann, J. C. Burant, S. Dapprich, J. M. Millam, A. D. Daniels, K. N. Kudin, M. C. Strain, O. Farkas, J. Tomasi, V. Barone, M. Cossi, R. Cammi, B. Mennucci, C. Pomelli, C. Adamo, S. Clifford, J. Ochterski, G. A. Petersson, P. Y. Ayala, Q. Cui, K. Morokuma, D. K. Malick, A. D. Rabuck, K. Raghavachari, J. B. Foresman, J. Cioslowski, J. V. Ortiz, B. B. Stefanov, G. Liu, A. Liashenko, P. Piskorz, I. Komaromi, R. Gomperts, R. L. Martin, D. J. Fox, T. Keith, M. A. Al-Laham, C. Y. Peng, A. Nanayakkara, C. Gonzalez, M. Challacombe, P. M. W. Gill, B. G. Johnson, W. Chen, M. W. Wong, J. L. Andres, M. Head-Gordon, E. S. Replogle, J. A. Pople, Gaussian, Inc., Pittsburgh, PA, **1998**.
[27] J. P. Ryckaert, G. Ciccoti, H. J. C. Berendsen, *J. Comput. Phys.* **1977**, *23*, 327–341.
[28] T. A. Darden, D. York, L. G. Pedersen, *J. Chem. Phys.* **1993**, *98*, 10089–10092.
[29] CCDC-846723 (**9**) and CCDC-854932 (**15**) contain the supplementary crystallographic data for this paper. These data can be obtained free of charge from The Cambridge Crystallographic Data Centre via www.ccdc.cam.ac.uk/data_request/cif.
[30] G. M. Sheldrick, SHELXL97. Program for the refinement of crystal structures, University of Göttingen, Germany, **1997**.

Received: October 3, 2011
Revised: January 19, 2012
Published online: March 1, 2012

  